Microwave-assisted dehydration of fructose and inulin to HMF catalyzed by niobium and zirconium phosphate catalysts

Claudia Antonetti [a,b], Mattia Melloni [c], Domenico Licursi [a], Sara Fulignati [a], Erika Ribechini [a], Sandra Rivas [d], Juan Carlos Parajó [d], Fabrizio Cavani [c,b], Anna Maria Raspolli Galletti [a,b,*]

[a] Department of Chemistry and Industrial Chemistry, University of Pisa, Via G. Moruzzi 13, 56124 Pisa, Italy
[b] Consorzio INSTM, Consorzio Interuniversitario Nazionale per la Scienza e Tecnologia dei Materiali, Via Giusti 9, 50121 Firenze, Italy
[c] Dipartimento di Chimica Industriale "Toso Montanari", University of Bologna, Viale Risorgimento 4, 40136 Bologna, Italy
[d] Department of Chemical Engineering, University of Vigo (Campus Ourense), As Lagoas, 32004 Ourense, Spain

ARTICLE INFO

ABSTRACT

5-Hydroxymethyl-2-furaldehyde (HMF) is a key bio-based platform for the production of renewable monomers and bio-fuels. However, most of its syntheses are carried out under not sustainable conditions. In this work, the production of HMF from fructose and inulin was investigated following the Green Chemistry principles, adopting aqueous medium, appreciable substrate concentration (10 wt%), low loading of heterogeneous acid catalyst (niobium or zirconium phosphate) and microwave heating. Both the catalysts resulted very active and promising, in particular zirconium phosphate and the performances were related to their different acid characteristics. The optimization of HMF synthesis with zirconium phosphate was also supported by a statistical modelling, which shows that the highest yield to HMF (about 40 mol%) is ascertained at high temperature (190 °C) and short reaction time (8 min). The catalysts resulted recyclable maintaining their starting activity almost unchanged.

© 2017 Elsevier B.V. All rights reserved.

1. Introduction

In the last years environmental problems, such as pollution, greenhouse effect and the dwindling supply of fossil materials, have driven the interest of the scientific community towards the valorisation of lignocellulosic biomass. This last represents a renewable, plentiful and cheap material for the industrial production, not only in the energy field but also as feedstock for the manufacture of chemicals, solvents and materials. This idea is included in the concept of "bio-refinery", which aims to a complete valorization of the lignocellulosic biomass to obtain an array of added-value products [1–11]. In this scenario 5-hydroxymethyl-2-furaldehyde (HMF) represents a key molecule, evaluated by the US Department of Energy as one of the most important bio-based compounds [12]. HMF is referred in the literature as a "sleeping giant" due to its high potentialities [13–16]. In fact, this platform chemical can be employed as an intermediate for the synthesis of a number of fine-chemicals, bio-fuels and monomers [10]. Some polysaccharides and monosaccharides, in particular fructose, represent the ideal starting materials for HMF synthesis [13–18]. Under acidic conditions, fructose undergoes a complex set of chemical reactions, leading to intermediates, HMF and reaction by-products. HMF is formed by fructose dehydration, and then is converted (at least in part) into by-products. HMF rehydration results in the formation of levulinic (LA) and formic (FA) acids, whereas humins are obtained from HMF polymerization [19,20]. These reactions are favoured by the presence of water, compelling many researchers to carry out the fructose dehydration in organic solvents [21–25], ionic liquids [26,27] and biphasic systems [28–31]. Considering safety, economic and environmental reasons, these solvents are less sustainable than water from the green chemistry perspective. Several mechanisms for the formation of HMF by acid-catalyzed dehydration of hexoses have been reported in the literature [15]. The mechanistic pathways can be divided in two groups. The first one assumes the reaction to proceed via acyclic intermediates, whereas the second type, largely reported in the literature, hypothesizes cyclic intermediates [32]. Scheme 1 shows the possible mechanism involving cyclic intermediates for the conversion of fructose to HMF and then to LA and FA. The dehydration of fructose is initiated by the proto-

* Corresponding author at: Department of Chemistry and Industrial Chemistry, University of Pisa, Via G. Moruzzi 13, 56124 Pisa, Italy.
E-mail address: anna.maria.raspolli.galletti@unipi.it (A.M. Raspolli Galletti).
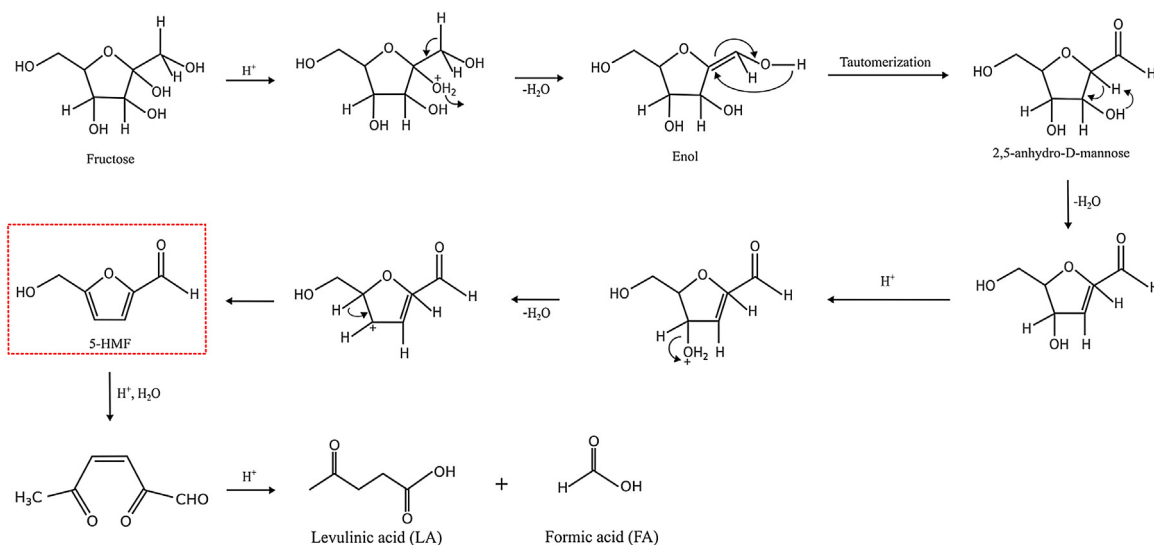
Scheme 1. Mechanism of fructose dehydration.

nation of the most basic hydroxyl group of the molecule, directly attached to the ring in the alpha position to the oxygen. The protonated form undergoes spontaneous dehydration and generates the cyclic intermediate enol, 2,5-anhydro-D-mannose, formed in the tautomerization step. The loss of water leads to the formation of HMF.

Both homogeneous and heterogeneous acid catalysts have been employed for the HMF synthesis but nowadays increasing research is focused on the use of heterogeneous ones. In fact, they are more suitable from an industrial perspective because avoid corrosion problems and facilitate catalyst separation and recycling. The most studied heterogeneous catalysts are ion-exchange resins [33,34], zeolites [35–37] and phosphates of transition metals (such as Nb, Zr, V, Cu, Ti) [38–45]. In particular, this last type of heterogeneous catalysts is very interesting because these systems keep their strong acidic properties in polar liquids [45], including water, also at high temperature [42,47,48]. Moreover, they can be easily reactivated by thermal treatments, as reported in the literature [45,49]. Carlini et al. [41] have carried out several studies regarding the fructose dehydration employing metal phosphates. They performed experiments on aqueous solutions containing 6 wt% of fructose at 100 °C in the presence of commercial niobium phosphate, employing substrate/catalyst ratio (RAC) from 1.4 to 1.7 wt/wt. Although the amount of catalyst was high, the reaction turned out to be slow but very selective, leading to 48 mol% conversion of fructose into HMF at 67 mol% selectivity. When they employed a more concentrated fructose solution (10 wt%), a decrease of HMF selectivity was ascertained. The same authors [40] investigated the fructose dehydration with zirconium and titanium phosphates under similar experimental conditions (100 °C, 6 wt% fructose in aqueous solution, RAC of 1.8 wt/wt) achieving higher HMF yields than those obtained with niobium phosphate, accounting for around 44 mol% for zirconium phosphate and 41 mol% for titanium phosphate. The same group considered the catalytic conversion of inulin into HMF under similar reaction conditions, reaching results similar to those reached from fructose. Recently, Zhang et al. [45] have studied the fructose dehydration, employing a synthetized niobium phosphate catalyst, working at 130 °C for 30 min with 8 wt% fructose in water. The authors reported high yields, up to 45 mol%, but adopting a too low substrate/catalyst ratio (1 wt/wt), which cannot be applied. Finally, Asghari et al. [38] claimed very high HMF yields, up to 50 mol%, when fructose was dehydrated for very short times, ranging from 60 s to 240 s, in aqueous medium using zirconium phosphate as a catalyst. However, also in this case, the adopted conditions are not acceptable from an applicative perspective because of the very low fructose concentration (1 wt%), and too low substrate/catalyst ratio (2 wt/wt).

On the other hand, microwave heating has recently become a fast growing research area because it can improve the efficiency of many processes. In fact, thanks to the interaction between the microwaves and the polar molecules, the heating starts from the core, resulting in faster temperature increase, thus reducing the reaction time and the energy consumption. Moreover, microwave irradiation enables a more efficient reaction control, generally affording higher yields of the target products [50–53].

In this context, now we have studied the catalytic dehydration of fructose and inulin to HMF in water adopting MW heating and heterogeneous acid catalysis. The effect of the main reaction parameters has been studied using two different heterogeneous catalysts (niobium and zirconium phosphate). To the best of our knowledge, this is the first work that reports the HMF synthesis in water under microwave heating with these catalytic systems.

2. Materials and methods

2.1. Materials

5-hydroxymethyl-2-furaldeyde (98%), formic acid (99,8%) and levulinic acid (98%) were purchased from Sigma-Aldrich and used as received. Fructose was food grade and used without any further purification. Inulin from *Dahlia Tubers* ($[\alpha]_D^{20} = -37.0$ and $M_n \approx 5000$) was purchased from Fluka and used as received. Niobium phosphate, kindly provided from CBMM (Companhia Brasileira de Metalurgia e Mineração), was treated at 255 °C for 6 h under high vacuum (5 Pa) before reaction.

2.2. Synthesis of zirconium phosphate

Zirconium Phosphate (ZrPO) was prepared as reported by Kamiya et al. [54] through the precipitation of $ZrOCl_2 \cdot 8H_2O$ (32 mL of 1 M aqueous solution) and $NH_4H_2PO_4$ (64 mL of a 1 M solution), at a molar ratio of P/Zr = 2. The precipitate was filtered, washed with water, dried at 100 °C, and calcined at 400 °C for 3 h before reaction.

2.3. Dehydration reaction

The dehydration reactions were carried out in a monomodal microwave reactor CEM Discover S-class System. In a standard reaction, aqueous fructose or inulin solutions (5 mL, 10% wt) were charged in the microwave reactor (10 mL) with the proper amount of the catalyst. The vessel was placed in the chamber of the MW reactor and heated at the desired temperature for the selected time under magnetic stirring. At the end of the reaction, the vessel was cooled at room temperature through an external air flow that allows a fast cooling and a portion of the sample was taken for analysis. The sample was filtered through a syringe filter (Whatman 0.45 μm PTFE) and analysed using a high-performance liquid chromatograph Perkin Elmer Flexer Isocratic Platform equipped with a column Benson 2000-0 BP-OA (300 mm × 7.8 mm) kept at 60 °C, employing 0.005 M H_2SO_4 as a mobile phase (flow-rate, 0.6 mL/min). The concentrations of the products were determined from calibration curves obtained with standard solutions. Fructose conversion, yield and selectivity was expressed in moles%. The unidentified products include humins, other soluble and insoluble compounds and gases. Their yield (mol%) was determined through the following equation: [(converted fructose moles – HMF moles – FA moles)/starting fructose moles] × 100. Starting from one mole of fructose, the dehydration reaction leads to one mole of HMF, and further HMF rehydration generates formic and levulinic acids in equimolar amounts. All the experiments were carried out in triplicate and the reproducibility of the technique was within 5%. For the recycle test, the used catalyst was recovered by filtration, washed with acetone and reused in two successive reactions. The washing solutions of the used catalysts were concentrated, dried under nitrogen flow and then analyzed by EGA-MS and Py-GC/MS (see Section 2.5).

2.4. Analysis of catalyst properties

Ammonia-TPD characterization was carried out in order to determine the acidity of the catalysts used employing a Micromeritics TPDR Instrument. Samples were pretreated at 500 °C in He flow to remove contaminants. Then pulses of NH_3 (10% in He) were fed at 100 °C on the sample, until saturation. Then the sample was heated (at 10°/min) from room temperature up to 650 °C, and the desorption of ammonia was recorded by using a TC detector and a quadrupole MS. FT-IR spectra of pyridine adsorbed on samples were recorded according to the following procedure: first the pure sample was shaped in the form of a thin layer by pressing the powder at 10 ton/cm^2; then the sample was pretreated under vacuum (10^{-6} mbar) up to 500 °C (steps of 100 °C for 30′), and adsorption of pyridine was carried out under vacuum at room temperature. Finally, the sample was heated under vacuum at increasing temperatures (steps of 100 °C) up to 400 °C, and FT-IR spectra were recorded at the intermediate and final temperatures.

Gas-phase dehydration of ethanol was studied in order to investigate the surface acid properties of the two metals. The reaction was carried out in a fixed-bed reactor (20 mm i.d. × 30 cm length) continuously fed with gaseous ethanol at 15.6% v/v concentration in nitrogen flow, loading 400 mg of catalyst. The tests were performed in function of time at 250 °C, with a contact time of 0.4 s.

The gaseous flow exit from the reactor was analysed on-line with a micro-GC Agilent 3000A, equipped with an Agilent Plot Q column (stationary phase polystyrene-divinylbenzene) and an Agilent OV1 column (stationary phase 100% dimethylpolysiloxane).

The IR spectra of both fresh and spent catalysts were recorded in ATR mode with a Spectrum Two Perkin Elmer FT-IR spectrometer in the range of wavenumber 4000–450 cm^{-1}.

XRD analyses were carried out using a vertical goniometer diffractometer Philips PW 1050/81. The analyses were performed using the CuKα radiation, made monochromatic using a nickel filter, with λ = 0.15418 nm. The interval used was 5° < 2θ < 80°, with steps of 0.2°; the count of intensity was carried out every 2 s.

XRF analyses were performed employing a wavelength dispersive spectrometer Panalytical Axios Advanced equipped with tube rhodium and with a power of 4 kW.

Inductively Coupled Plasma Optical Emission Spectroscopy analyses (ICP-EOS) were carried out with a Spectro-Genesis instrument equipped with a software Smart Analyzer Vision.

Thermogravimetric analysis (TGA) was carried out in flowing air by means of a PerkinElmer TGA7 apparatus.

^{1}H NMR of 5-HMF in deuterated chloroform was carried out employing a Varian Gemini 200 BB spectrometer (200 MHz).

2.5. Extraction and purity grade of HMF

The isolated yield of 5-HMF obtained in run 9 was determined by continuous liquid/liquid extraction, adopting dichloromethane as extraction solvent on the aqueous reaction solution. The extraction proceeded for 4 h, then, dichloromethane was removed by distillation under reduced pressure and finally the isolated yellow solid was weighted. Finally, a little portion was dissolved in deuterated chloroform and analysed by ^{1}H NMR, and a purity grade of 94% was ascertained. Detailed ^{1}H NMR data (200 MHz, CDCl$_3$): δ = 2.99 ppm (s, 1H, −OH), 4.73 ppm (s, 2H, −CH$_2$OH), 6.53 ppm (d, 1H, −CH =), 7.21 ppm (d, 1H, −CH =), 9.59 ppm (s, 1H, −CHO).

On the basis of weighted amount and taking into account the purity grade of HMF, the isolated yield of HMF of 27.1 mol% for run 9 was obtained, while the HPLC-determined yield was 33.9 mol%. The same procedure was repeated for run 10 carried out in the presence of ZrPO obtaining the isolated yield of HMF of 29.6 mol% while the HPLC-determined yield of 36.6 mol%.

2.6. Statistical modelling

HMF synthesis in aqueous media, using ZrPO as catalyst was optimized using the response surface methodology (RSM). The set of experiments corresponded to an incomplete, factorial, centered experimental design. The selected independent variables and their respective variation ranges were established as follows: the substrate/catalyst ratio (RAC), 6–15 wt/wt; reaction time (t), 5–20 min; and temperature (T), 150–190 °C. For calculation purposes, the dimensionless and normalized variables, dimensionless substrate/catalyst ratio RAC (denoted x_1), dimensionless time (denoted x_2) and dimensionless temperature (denoted x_3), with variation ranges (−1, 1), were defined as follows:

$$x_1 = 2 \cdot [RAC(wt/wt) - 10.5]/(15-6) \tag{1}$$

$$x_2 = 2 \cdot [t(min) - 12.5]/(20-5) \tag{2}$$

$$x_3 = 2 \cdot [T(°C) - 170]/(190-150) \tag{3}$$

The structure of the experimental design allowed the development of empirical models, in which the dependent variables were evaluated as the sum of the contributions of the independent, dimensionless variables (including first order, interaction and second-order terms), according to the generalized expression:

$$y_j = b_{0j} + \Sigma_i b_{ij} x_i + \Sigma_i \Sigma_k b_{ikj} x_i x_k \tag{4}$$

where:

- y_j (j: 1–2) stand for the considered dependent variables,
- x_i or x_k (i or k: 1–3, k ≥ i) are the independent, dimensionless variables,
- b_{0j}....b_{ikj} are the regression coefficients, calculated from the experimental data by multiple regression using the least-squares method.

The considered dependent variables to define the chemical changes taking place in the media were as follows: y_1: fructose conversion, defined as moles of fructose converted/100 mol initial fructose; y_2: HMF yield, defined as moles HMF/100 mol of initial fructose; y_3: total yield in valuable products, defined as moles of HMF, FA and LA/100 mol of initial fructose. Their statistical significance was defined on the basis of a Student's t-test, the statistical parameters measuring the correlation (R^2) and the statistical significance of the models (based on the Fisher's F-test).

2.7. Analytical instrumentation

Evolved gas analysis-mass spectrometry (EGA-MS) measurements were carried out in a micro-furnace pyrolyzer (Multi-Shot EGA/PY-3030D Pyrolyzer, Frontier Lab) directly coupled with a 5973 Mass Selective Detector (Agilent Technologies, Palo Alto, CA, USA) single quadrupole mass spectrometer via a deactivated and uncoated stainless steel transfer tube (UADTM-2.5N, 0.15 mm i.d. × 2.5 m length, Frontier Lab). The temperature of the micro-furnace pyrolyzer was programmed from 50 °C to 800 °C at a heating rate of 12 °C/min under a helium flow (1 mL/min) with a split ratio 1:50. Samples of about 0.5 mg were placed into a steel sample cup. Py-GC/MS measurements were carried out in a micro-furnace pyrolyser (Multi-Shot EGA/PY-3030D Pyrolyzer, Frontier Lab). The pyrolysis temperature was 600 °C for a period of 20 s. Roughly 100–200 µg of each sample were put into a stainless steel cup and placed into the micro-furnace of the pyrolyser. The pyrolyser was connected to a gas chromatograph 6890 Agilent (USA) equipped with a split/splitless injector (used with a split ratio of 1:10 at a constant temperature of 280 °C), an HP-5MS fused silica capillary column (stationary phase 5% diphenyl and 95% dimethyl-polysiloxane, 30 m × 0.25 mm i.d., Hewlett Packard, USA) and a deactivated silica pre-column (2 m × 0.32 mm i.d., Agilent J&W, USA).

3. Results and discussion

3.1. Characterization of catalysts

Niobium phosphate (NbPO) and zirconium phosphate (ZrPO) are heterogeneous catalysts widely used for the conversion of renewable feedstocks due to their acidic properties, maintained also in polar media and at high temperature [46,48,54]. Several literature studies have been carried out to determine the acidic properties of metal phosphates catalysts. Studies have shown that the amorphous form of M^{4+} phosphates demonstrate higher activity due to increased overall acidity and surface area compared to their crystalline analogues [53,55,56]. Hattori et al. have investigated the source of the active sites on this class of catalysts. In their study on Zr phosphate, they concluded that the catalyst possesses weak and strong acid sites, deriving from P(OH) groups [57]. On the other hand, the Lewis acid centers could be attributed to Zr^{4+}, as suggested by Spielbauer et al. [58].

The nature of acid sites in the Nb phosphate supplied by CBMM has been deeply investigated. Recently Carniti et al. [47] confirmed the presence of both water-tolerant Lewis acid sites and residual Brønsted acid sites. Nb phosphate results a higher protonic solid than the well-known niobic acid catalyst [59]. Lewis acidity can be assigned to unsaturated Nb^{5+} sites, while Brønsted acidity is mainly originated by P–OH groups and, in lesser extent, by Nb–OH sites. The comparison of the acidity of ZrPO (surface area 108 m^2/g) and NbPO (133 m^2/g) samples was now performed by means of both NH$_3$-Thermal Programmed Desorption and FT-Infrared Transmission Spectroscopy after adsorption of pyridine vapours and desorption at increasing temperatures. Fig. 1 compares the NH$_3$-
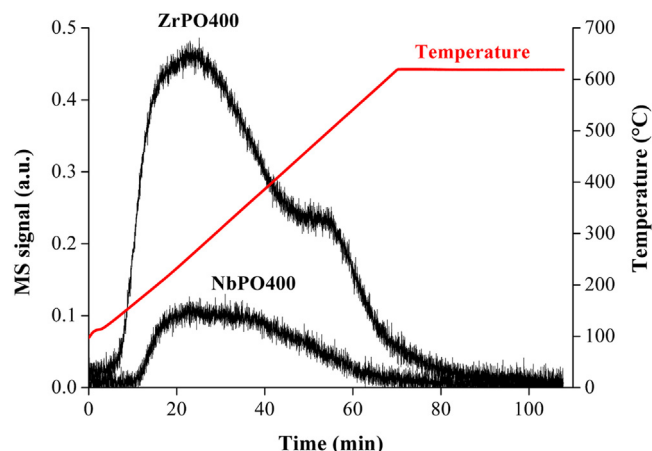

Fig. 1. NH$_3$-TPD profiles of ZrPO and NbPO calcined catalysts.

TPD profile of the two samples; they show similar profiles, with a predominant fraction of sites of low-medium strength and a relatively smaller fraction of stronger sites. However, the number of acid sites per unit weight is greater for the ZrPO catalyst, despite its lower surface area. Therefore, ZrPO holds a much greater aerial surface density of acid sites (measured as the number of sites/m^2) than NbPO.

Fig. 2 compares the transmission FT-IR spectra recorded at increasing temperatures for ZrPO and NbPO catalysts after room-T adsorption of pyridine (Fig. 2a) and after room-T adsorption of pyridine and water (Fig. 2b).

ZrPO catalyst displays a greater concentration of Lewis-type sites (L) (1450 cm^{-1}) which are of moderate strength. Conversely, in the case of NbPO, the Lewis sites are somehow stronger, since their concentration still is relevant even after treatment at 400 °C. The two samples show a similar concentration of Brønsted sites (B) (1545 cm^{-1}) of similar strength.

When pyridine and water were co-adsorbed, and the FT-IR spectra were registered after evacuation at increasing temperature, the two samples showed a different behavior, as shown in Fig. 2b. In the case of ZrPO, only a minor variation of the B/L intensity ratio was observed, compared to the case of pyridine-only adsorption. In the case of NbPO the concentration of L sites decreased and the one of B sites increased, with a relevant increase of the B/L ratio. Moreover, these B sites generated by water adsorption have a comparatively higher acidity. These data suggest that under hydrous conditions, NbPO is able to generate strong Brønsted-type acid sites. Conversely, in the case of ZrPO, acid sites seem to remain mainly of the Lewis type, whereas the B sites show a comparatively lower strength. A further insight of the type of surface acidity of the two phosphates in the presence of water was obtained by the gas-phase dehydration of alcohols. Fig. 3 shows the results achieved when a fixed-bed reactor was continuously fed with ethanol at 15.6% v/v concentration in nitrogen flow.

Tests were carried out in function of time, with a contact time of 0.4 s at 250 °C. The results show that, despite the higher number of acid sites (both per unit of weight and unit of surface area), ZrPO displays a lower activity than NbPO. Also the diethylether (DEE)/ethylene (E) yield ratio was very different in the two cases: close to 2.0 for ZrPO, but to 3.0–4.0 for NbPO. Brønsted acid sites are known to play an important role in the dehydration of ethanol to DEE and catalyst activity is closely related to acid strength [60]. Therefore, the higher activity and the higher DEE/E ratio shown by NbPO can be attributed to the stronger Brønsted-type acidity which is generated in-situ by interaction between Lewis sites and water formed by ethanol condensation and dehydration.

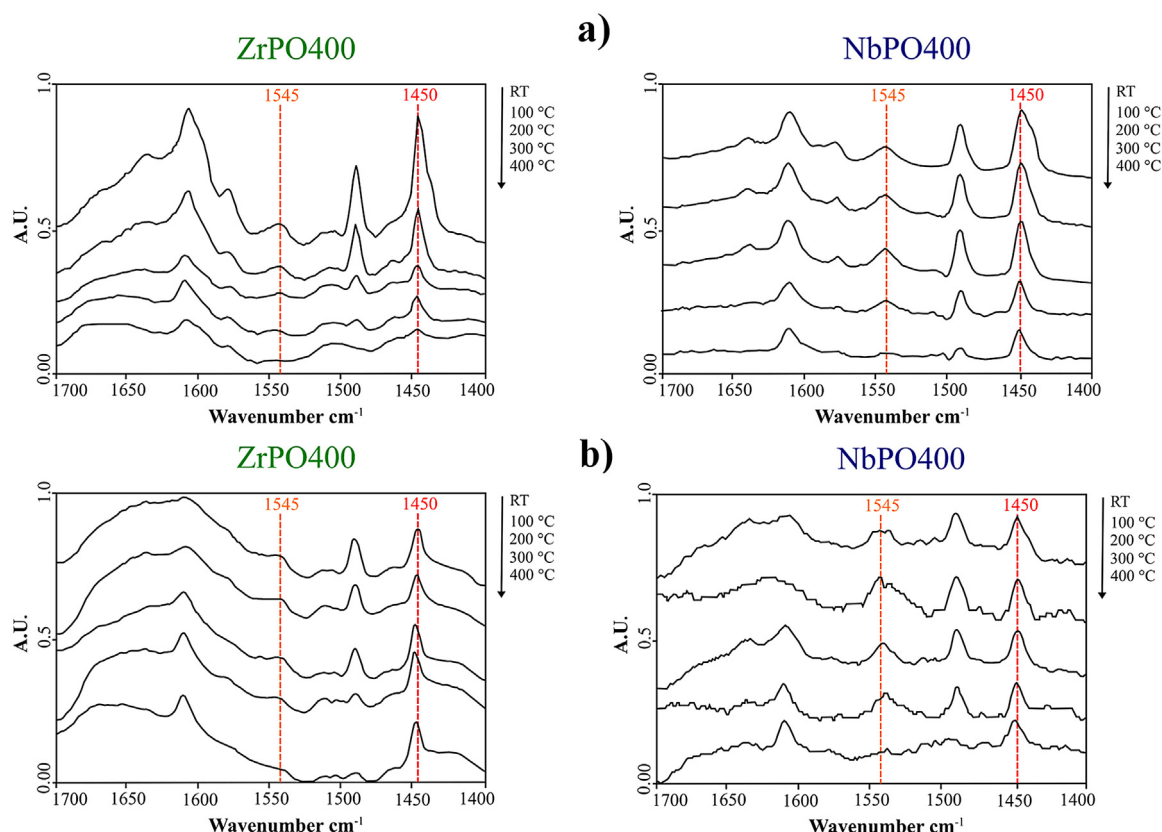The IR spectra of NbPO and ZrPO are reported in Fig. 4.

Fig. 2. (a) FT-IR spectra recorded at increasing temperatures after room-Temperature adsorption of pyridine over ZrPO and NbPO catalysts; (b) FT-IR spectra recorded at increasing temperatures after room-Temperature adsorption of pyridine and water over ZrPO and NbPO catalysts.

Broad bands at 1007 cm^{-1} and 1016 cm^{-1}, respectively of niobium phosphate and zirconium phosphate, can be assigned to asymmetric stretching of phosphate ion O=P=O [61]. Regarding the NbPO spectra, the second broad band at 591 cm^{-1} may be related to vibration of Nb–O bond, as already reported by Rocha et al. [62]. In the ZrPO spectra, instead, two adsorption bands can be identified: one at 510 cm^{-1} due to the asymmetric stretching of Zr–O bond, and one at 594 cm^{-1} due to the bending out of plane of P–OH bond [63]. Moreover bands at 3418 cm^{-1} and 1622 cm^{-1} are present in both spectra and related to adsorption of water on the catalyst surface [59].

The spectroscopic analysis of X-ray diffraction (XRD) allows us to determine the crystal structure and the nature of crystalline domains present in the catalysts. Fig. 5 shows the XRD spectra of the NbPO and ZrPO.

The XRD pattern of both samples shows two broad peaks in 2θ range of 10–40° and 40–70° indicating the amorphous nature of these phosphates.

The phosphorus (P)/metal (Zr or Nb) ratio present in the catalytic systems was determined by XRF analysis, resulting equal to 1.9 ± 0.1 and 0.33 ± 0.05 respectively for ZrPO and NbPO. Regarding ZrPO, the obtained ratio corresponds to the compound Zr(HPO$_4$)$_2$. This catalyst was previously reported as highly stable even in hydrolyzing conditions [53], and more active than crystalline compounds with similar composition, i.e., α-Zr(HPO$_4$)$_2$ and ζ-Zr(HPO$_4$)$_2$. The experimental P/Nb atomic ratio found for NbPO is in agreement with that reported by the CMBB (P/Nb atomic ratio 0.29).

3.2. Fructose conversion with niobium and zirconium phosphates

ZrPO and NbPO were employed in the HMF synthesis from a 10 wt% fructose aqueous solution. The fructose concentration

adopted in this work is higher than most concentrations reported in literature for aqueous systems [13–16]. Several parameters, such as amount of catalyst, temperature and reaction time, were investigated and the results are reported in Table 1.

A preliminary fructose dehydration experiment was performed in the absence of catalyst at 150 °C for 15 min under MW heating (run 1, Table 1). Under this condition, a negligible fructose conversion was achieved. On the other hand, the results obtained in the catalytic runs carried out at the same time and temperature (runs 2–6, Table 1) showed fructose conversions and HMF yields in the range of 47.6–90.4 mol% and 11.6–32.0 mol%, respectively, confirming the fundamental role of the catalyst. This role was better exerted adopting high amounts of the catalyst itself (RAC = 1.25–2.5). When RAC was increased up to 20 the yield to HMF significantly decreased and humins by-products prevailed. It is well-known that the acid-catalyzed decomposition of fructose is expected to proceed according to a number of series-parallel reactions [64], as shown in Scheme 2.

A kinetic modelling of this process in the presence of the adopted catalysts has not been performed and experimental activation energies are still unknown. Working at 150 °C with low NbPO loading the substrate decomposition (reaction 1, Scheme 2) seems prevailing. Indeed, run 6 carried out at the employed highest RAC value, equal to 20 wt/wt, shows the highest selectivity towards unidentified products. When the temperature was increased to 180 °C, higher formation of HMF and also of LA and FA was ascertained. This indicates a higher extent of reactions 2 and 4 (Scheme 2), which are significantly favoured by the increase of temperature. At higher temperature the increase of RAC from 5 to 10 (runs 7 and 8, Table 1) led to a slight decrease of fructose conversion but the selectivity to HMF was significantly improved (from 23.2 to 34.0 mol%). Correspondingly, the humins formation due to the reactions 1 and 3 dropped, due to the reduction of the amount of introduced stronger
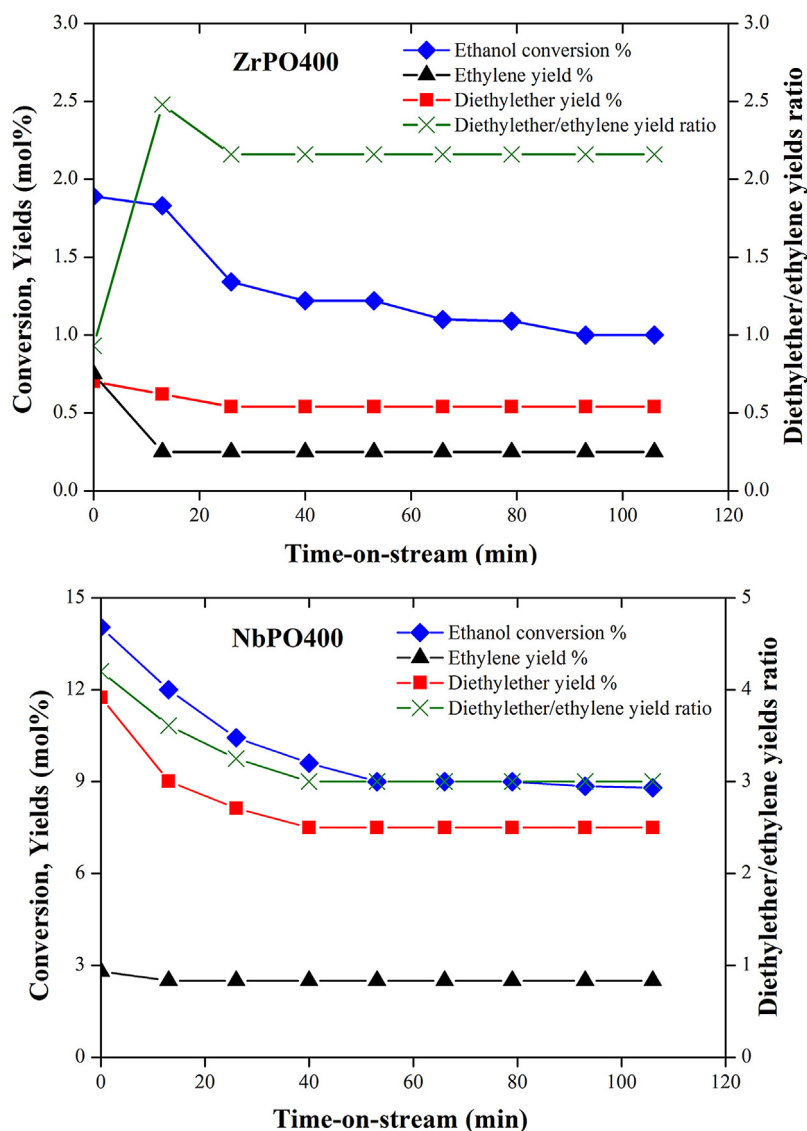
Fig. 3. Ethanol dehydration in gas-phase catalyzed by ZrPO and NbPO catalysts.

Table 1
Dehydration of aqueous fructose solutions (10% wt) to HMF in the presence of niobium phosphate and zirconium phosphate in different reaction conditions (RAC = substrate/catalyst ratio wt/wt).

Run	Cat	RAC	t (min)	T (°C)	Conv. (mol%)	HMF (mol%)		FA yield (mol%)	LA yield (mol%)	Unidentified products selectivity (mol%)
						Yield	Select			
1	Blank	/	15	150	4.2	2.5	60.0	0.0	0.0	40.5
2	NbPO	1.25	15	150	90.4	32.0	35.4	11.4	4.2	52.0
3	NbPO	2.5	15	150	75.4	27.4	36.3	trace	trace	63.7
4	NbPO	5	15	150	56.9	16.7	29.4	trace	trace	70.7
5	NbPO	10	15	150	54.8	15.3	27.8	trace	trace	72.1
6	NbPO	20	15	150	47.6	11.6	24.3	trace	trace	75.6
7	NbPO	5	15	180	95.9	22.2	23.2	13.6	5.2	62.7
8	NbPO	10	15	180	93.7	31.8	34.0	15.3	3.6	49.7
9	NbPO	10	10	180	86.5	33.9	39.2	13.3	2.0	45.4
10	ZrPO	10	10	180	76.4	36.6	47.9	11.2	0.7	37.4
11	ZrPO	7.5	10	180	84.2	39.5	47.0	13.3	2.4	37.3
12	Blank	/	10	180	35.3	16.8	47.6	trace	trace	52.4
13[a]	ZrPO	6	8	190	96.3	39.4	40.9	14.1	5.3	44.4
14[a]	NbPO	6	8	190	97.7	32.2	32.9	21.3	8.1	45.2

[a] Discussed in Section 3.3.
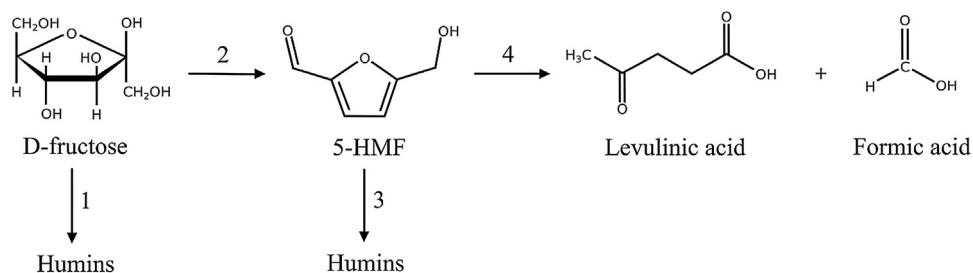
Scheme 2. Reaction network for the conversion of fructose to HMF.

Brønsted acid sites. Surely, the novelty of the results reported in this work, respect to those up to now shown in the literature, comes from the comparatively higher fructose concentration employed. In fact, the substrate concentration generally ranges from 1 wt% up to 6 wt%. Additionally, the substrate/catalyst ratio employed here is significantly higher than the one reported by other groups, which are usually in the range 1–5 wt/wt [13–16]. When run 9 was replicated in the presence of ZrPO, it resulted slightly less active, leading to a lower fructose conversion (run 10, Table 1). In fact, a substrate/catalyst ratio of 7.5 (run 11, Table 1) was needed to achieve a fructose conversion similar to that achieved in run 9 with NbPO. This can be ascribed to the fact that ZrPO presents a lower amount of strong Brønsted acidic sites (which are responsible for fructose dehydration) than NbPO, especially under hydrous conditions. Therefore, in comparison with NbPO, a greater amount of ZrPO was necessary to achieve similar fructose conversion and product yield. On the other hand, the experiments with ZrPO provided higher HMF yield and selectivity, with decreased generation of unidentified products. This result confirms that a milder Brønsted acid strength leads to a more selective formation of HMF. To assess the role of the catalyst at higher temperature, a blank run was performed at 180 °C for 10 min (run 12, Table 1). The reaction was slower than the catalytic runs carried out under the same experimental conditions in the presence of NbPO and ZrPO (runs 9 and 11 in Table 1), and a limited fructose conversion (35.3 mol%.) was achieved. These results confirm the efficiency of the catalysts for accelerating the reaction and for improving the HMF yield, in particular when ZrPO was employed. In this last case, the HMF selectivity was similar to the one attained in the blank run 12 (47.0 mol% in the catalytic test, and 47.6 mol% in the blank one, see Table 1).

From the collected results, it is possible to correlate the achieved catalytic performances of NbPO and ZrPO with the acid properties of these systems, hypothesizing that strong Brønsted acid sites are responsible for the fructose conversion, whereas medium strength Brønsted acid sites drive into a more selective formation of HMF. It must be emphasized that part of the interest of the results reported

in this work comes from the adopted experimental conditions. In fact, both NbPO and ZrPO catalysts have been widely tested in fructose dehydration to HMF, also by our research group, but under less sustainable conditions than those adopted in this work. Many authors carried out the reaction in organic medium [65] or in a biphasic system [49] in order to increase HMF selectivity, limiting rehydration reaction to levulinic acid and formic acid and polymerization reaction to humins [20]. However, these are not sustainable reaction media, due to their high boiling points that complicate HMF isolation, high cost and, sometimes, toxicity. In this work, water is employed as reaction solvent even if it leads to lower HMF selectivity because it is the greenest inexpensive solvent, without drawbacks for environment and health. On the other hand, the most important investigations adopting aqueous medium and reaction conditions near to those adopted by us in this work are summarized in Table 2 [38,40,41,45].

All these works adopt low fructose concentrations (under 8 wt%), and, above all, low RAC value (under 2 wt/wt). It is well known that an increase of the substrate concentration leads to a drop of HMF yield due to a greater humins formation [21] and the achievement of high HMF yield starting from concentrated substrate solution is still an unsolved challenge. On the other hand, high loadings are necessary for industrial application, making easier and cheaper the product recovery. In this perspective, the yields obtained in this work (up to 33.9 mol% with NbPO and 39.5 mol% with ZrPO) are of great relevance, because they are similar to those reported in literature but reached starting from much more concentrated fructose solutions (10 wt%) and with a higher RAC (10 wt/wt for NbPO and 7.5 wt/wt for ZrPO).

In the literature, the dehydration of fructose with niobium phosphate is also reported in a flow reactor. Carniti et al. [42] carried out the reaction at temperature between 90 and 110 °C continuously feeding a 5 wt% fructose aqueous solution, changing the flow rate in order to have contact times from 5 to 55 min g ml^{-1}. Under the best experimental conditions, they reached a HMF yield around 26 mol%, which is lower than that reported in this work, notwithstanding it was obtained starting from a lower concentrated fructose solution.

On the basis of the comparatively better results obtained using ZrPO, an in-depth study regarding the optimization of HMF synthesis with this catalyst was carried out.

3.3. Optimization of HMF synthesis from fructose through statistical modelling

HMF synthesis from fructose using ZrPO as a catalyst under microwave heating depends on a large number of variables. In complex problems like this, where the target variables depend on a number of independent factors, the Response Surface Methodology (RSM) may be a useful tool for achieving a quantitative interpretation of the studied phenomena using experimental plans affordable in terms of experimental work. The assessment started with the identification of the most influential parameters on fructose conversion, which were employed as independent variables in the
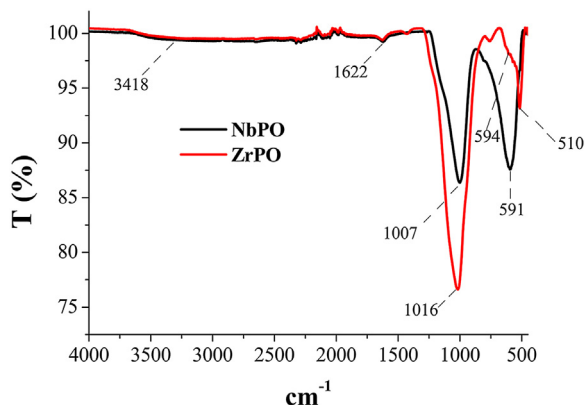

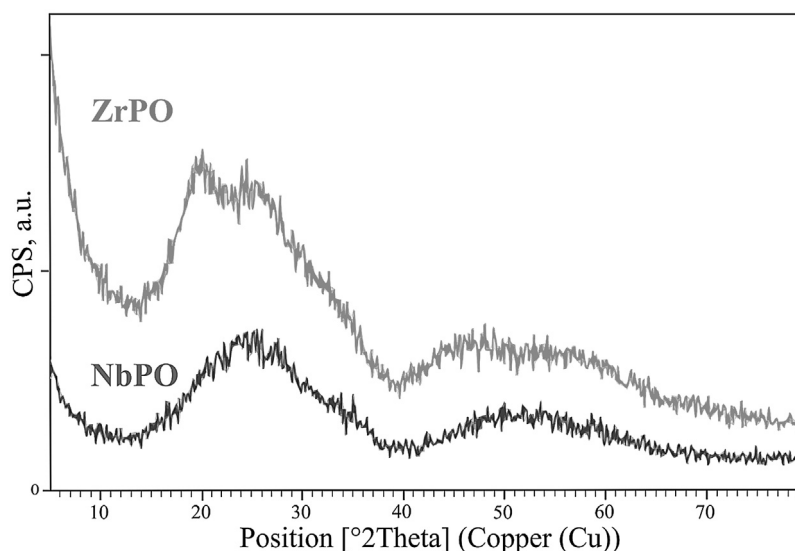**Fig. 4.** FT-IR spectra recorded in ATR mode of NbPO and ZrPO.

Fig. 5. XRD patterns of NbPO and ZrPO.

Table 2
Reaction conditions and HMF yields obtained in water from literature investigations.

Literature Reference	Cat	T (°C)	t (min)	Fructose loading (wt%)	RAC (wt/wt)	HMF yield (mol%)
[41]	NbPO	100	360	6%	1.4–1.6	30%
[45]	NbPO	130	30	8%	1	45%
[40]	ZrPO	100	60	6%	1.8	44%
[38]	ZrPO	240	2	1%	2	50%
[40]	TiPO	100	60	6%	1.8	41%

Table 3
Operational conditions defining the experiments assayed for HMF production from fructose using ZrPO as catalyst, expressed in terms of dimensional and dimensionless variables and concentrations of fructose and reaction products (HMF, FA and LA).

Run	Dimensionless normalized variables			Dimensional variables			Concentrations (mmol/L)			
	x_1	x_2	x_3	RAC (w/w)	t (min)	T (°C)	Fructose	HMF	FA	LA
D1	−1	−1	−1	6	5	150	390.1	16.3	0.0	0.0
D2	−1	1	−1	6	20	150	323.7	61.7	0.0	0.0
D3	−1	−1	1	6	5	190	84.9	202.7	41.6	18.0
D4	−1	1	1	6	20	190	7.6	130.3	82.9	53.9
D5	1	−1	−1	15	5	150	394.3	8.2	0.0	0.0
D6	1	1	−1	15	20	150	353.4	55.0	0.0	0.0
D7	1	−1	1	15	5	190	124.7	194.2	27.9	10.3
D8	1	1	1	15	20	190	8.8	141.6	69.1	41.1
D9	−1	0	0	6	12.5	170	125.9	155.8	27.9	10.3
D10	1	0	0	15	12.5	170	157.7	131.7	27.9	2.6
D11	0	−1	0	10.5	5	170	351.8	65.0	0.0	0.0
D12	0	1	0	10.5	20	170	94.3	155.8	27.9	12.9
D13	0	0	−1	10.5	12.5	150	358.1	36.1	0.0	0.0
D14	0	0	1	10.5	12.5	190	16.9	189.9	55.4	28.3
D15	0	0	0	10.5	12.5	170	170.4	130.3	27.9	5.2
D16	0	0	0	10.5	12.5	170	184.4	148.7	0.4	0.0
D17	0	0	0	10.5	12.5	170	152.8	154.4	27.9	5.2

statistical design RAC, t, and T. The initial fructose concentration (10 wt%) and the type of catalysts, were fixed variables on the basis of previous studies. In the same way, the ranges considered for the independent variables selected in this study were established on the basis of preliminary assays. Table 3 shows the operational conditions assayed in the experiments making part of the experimental design, the independent variables and the detailed data of concentration valuable products.

As mentioned above, the dependent variables considered to measure the chemical changes taking place in the media were y_1, fructose conversion; y_2, HMF yield, and y_3, total yield in valuable

products shown in Table 4. Y_3 was defined as the sum of the molar concentration of HMF, FA and LA formed per 100 mol of substrate.

According to the data in Tables 3 and 4, fructose conversion resulted in HMF generation, whereas the formation of measurable amounts of organic acids (LA and FA) took place just under conditions of intermediate or high severity. The experiments performed at 150 °C resulted in limited fructose conversions and no formation of LA and FA (Tables 3 and 4). The almost complete fructose consumption was achieved under harsh conditions (Tables 3 and 4, run D4). The highest concentrations of FA and LA were also achieved under the severest conditions considered (Tables 3 and 4). Severer conditions would be necessary to achieve higher yields of FA and

Table 4
Experimental conversion of fructose (y_1), and experimental HMF yield (y_2) and the total molar yield of valuable products (y_3,) (see Table 2 for operational conditions corresponding to a given experiment).

Run	y_1 (%)	y_2 (%)	y_3 (%)
D1	29.7	2.9	2.9
D2	41.8	11.1	11.1
D3	84.7	36.5	47.3
D4	98.6	23.5	48.1
D5	29.0	1.5	1.5
D6	36.4	9.9	9.9
D7	77.6	34.9	40.5
D8	98.4	25.5	45.4
D9	77.4	28.0	35.0
D10	68.5	23.0	29.2
D11	36.7	11.7	11.7
D12	83.0	28.1	35.4
D13	35.5	6.5	6.5
D14	97.0	34.2	49.3
D15	69.3	23.5	29.4
D16	66.8	26.8	26.9
D17	72.5	27.8	33.8

LA, but this is not the major focus of this study, which is direct towards the optimization of HMF production.

Concerning the RSM modelling of data, Table 5 lists the values calculated for the set of regression coefficients involved in the equations describing the behavior of the dependent variables y_1, y_2 and y_3, as well as their statistical significance on the basis of a Student's t-test. The same Table includes the statistical parameters measuring the correlation (R^2) and the statistical significance of the models (measured by the Fisher's F parameter).

The coefficients calculated for the fructose conversion y_1 confirmed that this variable was significantly affected by time and temperature, the major effects being caused by this latter; whereas no significant effects were caused by substrate/catalyst ratios within the tested range. Increased temperatures and/or reaction times improved the substrate consumption, which presented a wide variation range (from values below 30% in experiments performed under mild conditions up to almost quantitative consumption under harsh conditions). The response surface calculated for y_1 operating at the intermediate amount of catalyst ($x1 = 0$) is shown in Fig. 6: fructose conversions >90% were predicted at 190 °C for reaction times >9 min, or at 184 °C for more than 15 min. Near total conversion was predicted for the severest conditions considered (190 °C, 20 min).

Table 5
Regression coefficients ($b_{0j} . . . b_{33j}$) and statistical parameters measuring the correlation and significance of models.

Parameter	Variable		
	y_1	y_2	y_3
b_{0j}	69.06[b]	24.99[b]	29.49[b]
b_{1j}	−2.235	−0.725	−1.792
b_{2j}	10.05[b]	1.050	4.608[a]
b_{3j}	28.39[b]	12.27[b]	19.85[b]
b_{12j}	0.289	0.485	0.538
b_{13j}	−0.159	0.392	−0.858
b_{23j}	1.923	−4.882[a]	−1.356
b_{11j}	4.202	1.264	2.986
b_{22j}	−8.853	−4.350	−5.539
b_{33j}	−2.473	−3.870	−1.206
Multiple correlation coefficient	0.975	0.959	0.981
R^2	0.951	0.922	0.962
Adjusted R^2	0.887	0.821	0.914
F exp.	15.02	9.142	20.00

[a] Coefficients significant at the 95% confidence level.
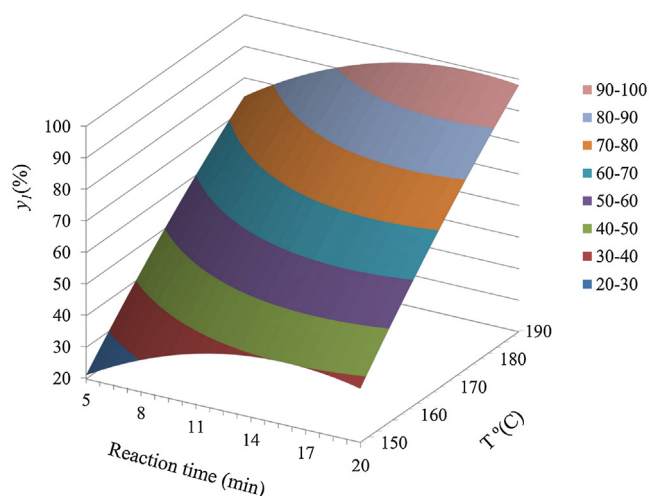[b] Coefficients significant at the 99% confidence level.

Fig. 6. Dependence of the fructose conversion (variable y_1) on temperature and time, calculated for the intermediate substrate/catalyst ratio ($x_1 = 0$).

The yield in HMF (variable y_2) is mainly dependent on temperature, and the model also shows a significant time-temperature interaction term (Table 4). Fig. 7a shows the calculated dependence of y_2 on RAC and T for treatments at the intermediate reaction time, whereas Fig. 7b shows the dependence of y_2 on RAC and time, at 190 °C.

Both figures show that a variation of the substrate/catalyst ratio hardly affects the yield of HMF. Fig. 7c shows the response surface calculated for y_2 as function of t and T for $x_1 = −1$. For a given reaction time, higher temperatures improve the HMF yield, but at 190 °C, reaction times >11 min promote HMF decomposition. The highest HMF yields (above 34 mol%) is predicted at 190 °C for reaction times in the range 6.5–11 min. This finding is in agreement with the comparatively high HMF yields obtained in experiments D3, D7 and D14 of Tables 3 and 4 (all of them performed at the highest temperature assayed). The experimental model predicts a maximal HMF yield of 36.1 mol% in the optimal conditions: 190 °C for 8.8 min and an RAC = 6 wt/wt. Under these conditions, the experimental value of yield for HMF was 39.4 mol% (run 13, Table 1), confirming the good prediction of the model. The fructose dehydration with NbPO in the same experimental conditions was also carried out and a yield to HMF of 32.2 mol% was achieved (run 14, Table 1). Oppositely, higher yields of FA and LA (21.3 mol% and 8.1 mol%, respectively) were achieved. Improved HMF yields at high temperatures have been reported in literature [66]. Rivas et al. [67] found that higher HMF concentrations from hexoses were achieved at higher temperatures, since this variable caused more marked effects on the reactions leading to HMF production than on the reactions involved in HMF decomposition. Concerning the total yield in valuable products (variable y_3), Fig. 8 shows the surface response calculated for this variable as a function of temperature and time for RAC fixed in its minimum value. The major experimental trends observed for y_3 are closely related to the ones determined for the HMF yield, particularly regarding the beneficial effect of temperature. It can be noted that the maximum total yield of valuable products (54%) was predicted for the same temperature than the maximum HMF yield (190 °C), but for a longer reaction time (14.3 min in comparison with 8.8 min).

3.4. Concentration profiles for HMF production from fructose in aqueous media under microwave irradiation

Fig. 9 shows the time concentration profiles determined when fructose was treated in aqueous media under microwave irradi-
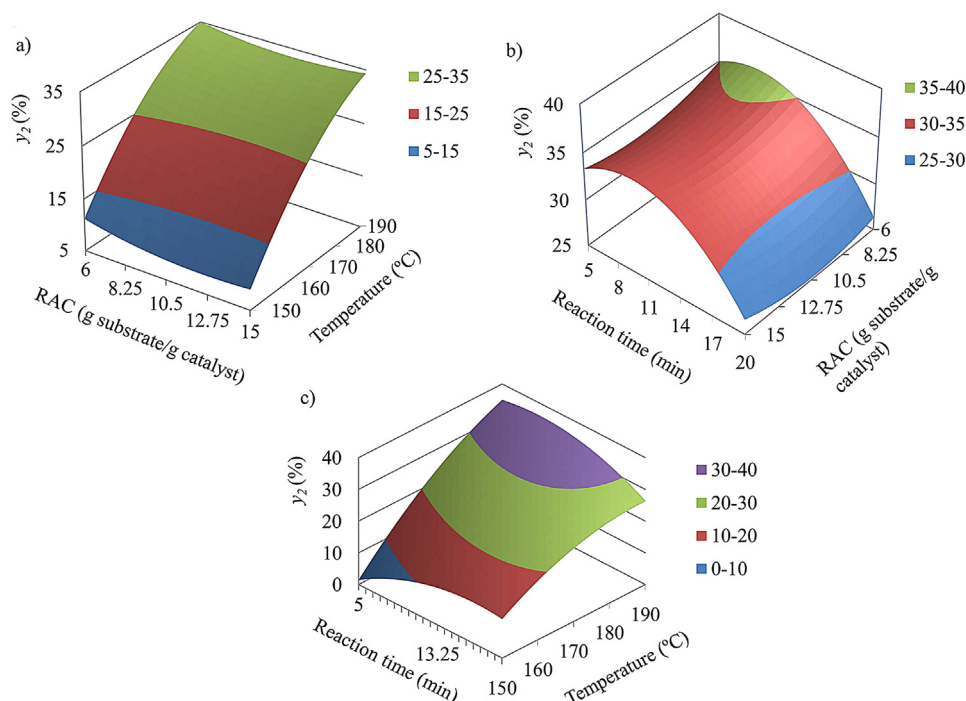
Fig. 7. Dependence of the HMF yield (variable y_2) on the: (a) substrate/catalyst ratio and temperature, calculated for the intermediate time (($x_2 = -0$); (b) reaction time and substrate/catalyst ratio calculated for the maximum temperature assayed (($x_3 = 1$); (c) temperature and time, calculated for the substrate/catalyst ratio of 6 ($x_1 = -1$).

ation using ZrPO as a catalyst, operating at the best temperature (190 °C) and substrate/catalyst ratio (6) identified in the RSM study.

The initial fructose concentration was 10 wt% (or 555 mmol/L). The substrate was consumed in part during the heating of the reaction media. When the target temperature was reached, 63% of the initial amount of fructose remained in the medium. Fructose conversion proceeded with a fast kinetics during the first reaction stages (lasting about 10 min), leading to the formation of HMF, FA and LA. The highest HMF concentration was achieved in the 6 and 15 min, with a maximum experimental yield of 39.3 mol% after 8.8 min. The HMF concentration dropped markedly for reaction times longer than 15 min, owing to the predominant effects of side reactions leading to the consumption of the target prod-

uct. Concerning the concentration profiles determined for FA and LA, both of them are fairly linear, with similar slope but different ordinate. As it can be seen in Fig. 9, significant amounts of FA were formed during the heating-up period, but no significant generation of LA took place. This could be ascribed to side reactions that lead to the formation of FA and other compounds [68,69]. When the target temperature was achieved, the generation of FA and LA was fairly equimolar, following the stoichiometry of the HMF rehydration reaction.

3.5. HMF synthesis from inulin

Inulin is a polysaccharide made up of fructose structural units, which is present in many plants and is industrially produced from chicory. A number of polysaccharides, including inulin, have been used in literature as feedstocks for HMF production, because they can be hydrolyzed into monosaccharides (the true HMF precursors) [70]. On the basis of the results obtained for HMF manufacture from fructose in the presence of NbPO and ZrPO, the same reaction media were assayed for producing HMF from inulin. Considering that the kinetics of inulin hydrolysis was faster than the dehydration of fructose into HMF, reactions with inulin were carried out under the optimal experimental conditions found for each of the catalysts assayed. Table 6 lists the results achieved starting from inulin using NbPO and ZrPO working at 180 °C for 10 min with a substrate/catalyst ratio of 10 for NbPO (run 17, Table 6) and at 190 °C for 8 min with a substrate/catalyst ratio of 6 for ZrPO (run 18, Table 6). For comparison, the results achieved with fructose under the same conditions are also included in the same Table (runs 9 and 13), together with the blank experiments performed at 180 °C for 10 min and at 190 °C for 8 min.

Inulin was completely converted in all the experiments, as it was expected owing to its high susceptibility to hydrolysis. Regardless the catalyst employed, high fructose conversions were achieved, and the HMF yields were similar to those obtained using fructose as a substrate. In the presence of niobium phosphate, the yields of
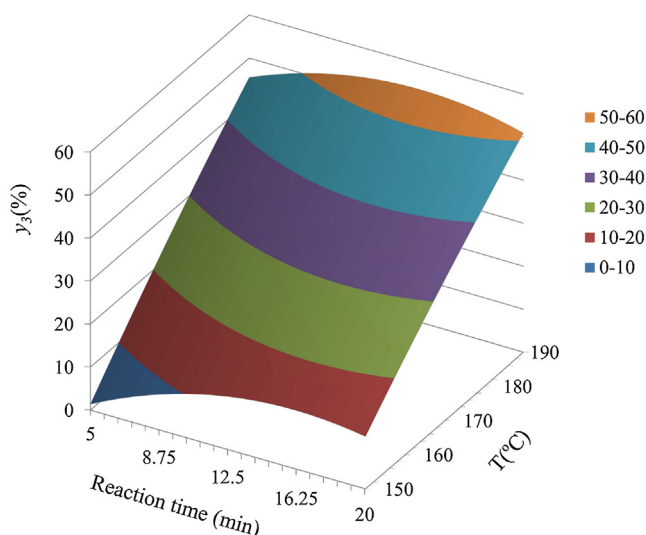

Fig. 8. Dependence of the total yield in valuable products (variable y_3) on temperature and time, calculated for the substrate/catalyst ratio $x_1 = -1$.

Table 6
Comparison between fructose and inulin aqueous solutions (10% wt) as substrate in dehydration reactions with niobium phosphate and zirconium phosphate and inulin blank runs (the conversion of inulin was always complete).

Run	Cat	Substr.	Experimental Conditions			Conv. Fruct. (mol%)	HMF (mol%)		FA yield (mol%)	LA yield (mol%)	Unidentified products selectivity (mol%)
			T °C	t min	RAC		Yield	Select			
15	Blank	inulin	180	10	/	38.0	13.8	36.3	trace	trace	59.5
16	Blank	inulin	190	8	/	45.9	16.6	36.2	3.1	1.8	57.1
9	NbPO	fructose	180	10	10	86.5	33.9	39.2	13.3	2.0	45.4
17	NbPO	inulin	180	10	10	92.5	33.4	36.1	14.9	3.2	45.5
13	ZrPO	fructose	190	8	6	96.3	39.4	40.9	14.1	5.3	44.4
18	ZrPO	inulin	190	8	6	98.1	42.1	42.9	6.5	2.3	50.5

Table 7
Dehydration reaction of fructose in the presence of NbPO (reaction conditions: T = 180 °C; t = 10 min; RAC = 10 wt/wt) and ZrPO (reaction conditions: T = 190 °C; t = 8 min; RAC = 6 wt/wt) and two subsequent recycles of the solid catalysts.

Run	Cat	Conv. (% mol)	HMF (% mol)		FA yield (% mol)	LA yield (% mol)	Unidentified products selectivity (% mol)
			Yield	Select			
9	Fresh NbPO	86.5	33.9	39.2	13.3	2.0	45.4
9bis	Used NbPO	84.8	31.8	37.5	12.9	2.0	47.3
9tris	Used NbPO	83.8	30.1	35.9	12.6	1.8	49.0
13	Fresh ZrPO	96.3	39.4	40.9	14.1	5.3	44.4
13bis	Used ZrPO	94.5	38.3	40.5	13.8	5.1	44.8
13tris	Used ZrPO	92.7	36.1	38.9	13.5	4.9	46.5

FA and LA and the generation of unidentified products were similar to those obtained from fructose. Some differences in the distribution of by-products were observed when inulin or fructose were reacted in the presence of ZrPO, particularly regarding the FA yield (which was higher in experiments from fructose) and the selectivity in unidentified products (which was lower for the same substrate). In order to assess the improvements derived from the presence of catalysts, blank runs were performed (runs 15 and 16, Table 6). At the end of the reactions, inulin was not detected, confirming its high susceptibility to hydrolysis. A significant amount of unreacted fructose was detected at the end of reactions, and the corresponding HMF yields were much lower than the ones achieved in catalyzed conditions.

In conclusion, high HMF yields can be obtained from inulin under the reaction conditions just identified for the fructose dehydration, confirming the relevance of the catalytic approach in comparison with autohydrolysis for higher substrate concentrations.

3.6. Stability and catalyst recyclability

Since the stability of the catalysts is of great importance in an applicative perspective, their recyclability has been investigated. NbPO from run 9 and ZrPO from run 13 (see Table 1) were recovered by filtration, washed with acetone and reused in two successive reactions carried out under the same conditions of the first cycle. The results are reported in Table 7.

The obtained results confirm the feasibility of catalyst reactivation by simple washing. In fact, for both NbPO and ZrPO, only a slight decrease both in fructose conversion and HMF selectivity was observed. The good efficiency of the washing method suggests that the most of polymers, probably deriving from condensation reactions, are soluble ones, easily removed by acetone. A preliminary study of the molecules released in these washing solutions carried out employing EGA-MS and Py-GC/MS analyses recognized furanic, benzofuranic and aromatic compounds along with benzofurans and polyaromatics as main pyrolysis products. These evidences suggest the presence of still condensed compounds, however removable with the washing procedure. The straightforward identification of such polymers is under further investigation. In addition, the leaching of both metals, Nb and Zr, in the reaction media obtained at the end of the catalytic runs was ascertained by ICP analysis. Under the employed experimental conditions, NbPO and ZrPO show negligible metal leaching, thus allowing us to exclude any dissolution of Nb and Zr in the aqueous phase. On the other hand, in previous work of ours, we also verified the release of P of the ZrPO catalyst used for lignocellulosic hydrolysis under conventional conditions [54]. It was reported that the fresh catalyst releases P during the first experiment (there was no dissolution of Zr), a phenomenon which could explain the slight decline of activity during repeated uses of the catalyst. However, it was also demonstrated that the low amount of P released during the first use did not contribute to the catalytic behavior experimentally observed for the fresh ZrPO catalyst.

In order to verify the presence of organic deposits on the spent catalysts, FT-IR analysis of NbPO and ZrPO recovered at the end of the reactions run 9 and 10 respectively was conducted. The recorded spectra were compared with those of fresh catalysts in Fig. 10.

The spectra of spent catalysts show characteristic bands of soluble or insoluble humins proving that organic deposits are present on catalysts surface. In fact, bands at $1705\,cm^{-1}$, $1517\,cm^{-1}$, $1370\,cm^{-1}$ and $1279\,cm^{-1}$ can be identified both in spent NbPO and ZrPO spectra and assigned respectively to stretching of C=O of carbonyl groups, stretching of C=C in furan and/or aromatic compounds, stretching of C—O—C bond of furan ring and stretching of C—O bond of ethers [71–74]. In addition, the spectrum of the used catalyst ZrPO shows two others bands: one at $1664\,cm^{-1}$, due to stretching of C=O of quinones, and one at $802\,cm^{-1}$ due to bending out of plane of =C—H bond of aromatic and/or furan rings [74]. Moreover, the characteristic bands of phosphates result less intense in the spectra of spent catalysts than the corresponding ones of the fresh samples, maybe because the organic deposits make the catalyst surface less available to the IR radiation.

In Fig. 10 the IR spectra of NbPO and ZrPO after the washing treatment are also reported. It is interesting to highlight that the IR spectra of the catalysts after the acetone washing are very similar to those of the fresh samples, thus confirming the feasibility of this simple reactivation method, as indirectly suggested by the recycle tests.
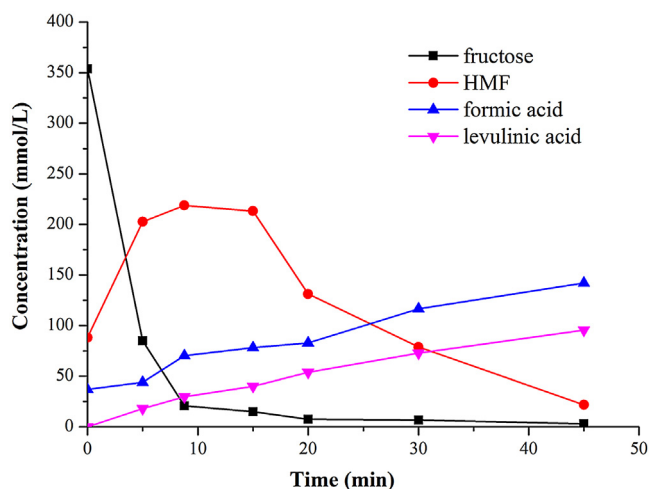
Fig. 9. Concentration profiles determined for the fructose, HMF, formic acid and levulinic acid, operating in microwave system, in water at 190 °C using ZrPO as catalyst in RAC = 6 wt/wt. Initial amount of fructose: 555 mmol/L.
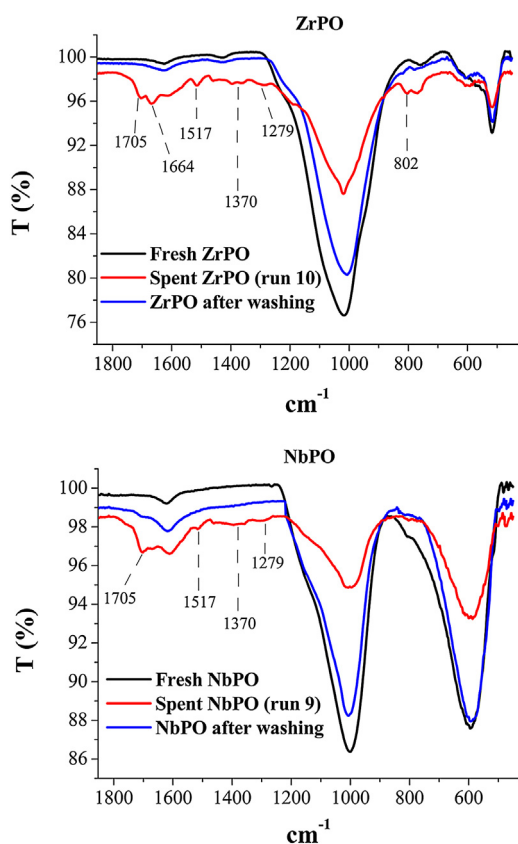

Fig. 10. Comparison between FT-IR spectra of fresh catalyst, spent catalyst and catalyst after washing reactivation for NbPO and ZrPO, in wavenumber range of 1850–430 cm^{-1}.

Moreover, TGA analysis was performed on spent catalysts recovered at the end of the reactions run 9 and 10 and both samples, when heated in air flow, show a weight loss close to 11% until 400 °C; loss is complete at this temperature. This indicates that organic residues can be removed by means of a mild oxidizing treatment. Therefore both catalysts result stable and suitable solid acid systems for catalysis in water.

4. Conclusions

The dehydration of fructose to HMF with NbPO and ZrPO under sustainable conditions was investigated. These catalysts present different acidic properties both for amount of total acidic sites, for Brønsted/Lewis acid site ratio and for their strength. The two catalysts showed a different catalytic behavior: NbPO turned out to be more active than ZrPO in fructose conversion, despite the overall amount and density of acid sites were considerably lower than those of ZrPO. This was due to the fact that under hydrous conditions the Lewis sites of NbPO interacted with water and developed stronger Brønsted sites than ZrPO, whose acid features were instead substantially unchanged under both anhydrous and hydrous conditions. On the other hand, ZrPO was more selective to HMF than NbPO, which can be addressed to the predominance of medium-strength Brønsted sites while stronger acid sites promote the formation of undesired heavy compounds.

Therefore, ZrPO results more promising than NbPO, leading to higher HMF yields. The optimization of HMF synthesis with ZrPO was also carried out through a statistical modelling, which shows that the highest HMF yield (39.4 mol%) is ascertained at high temperature (190 °C) and at short times (8 min). Comparable results were obtained starting from inulin.

References

[1] R. Luque, K. Triantafyllidis, Valorization of lignocellulosic biomass, ChemCatChem 8 (2016) 1422–1423.
[2] C. Antonetti, E. Bonari, D. Licursi, N. Nassi o Di Nasso, A.M. Raspolli Galletti, Hydrothermal conversion of giant reed to furfural and levulinic acid: optimization of the process under microwave irradiation and investigation of distinctive agronomic parameters, Molecules 20 (2015) 21232–21253.
[3] A. Galia, B. Schiavo, C. Antonetti, A.M. Raspolli Galletti, L. Interrante, M. Lessi, O. Scialdone, M.G. Valenti, Autohydrolysis pretreatment of Arundo donax: a comparison between microwave-assisted batch and fast heating rate flow-through reaction systems, Biotechnol. Biofuels 8 (2015) 218–236.
[4] R. Luque, Catalytic biomass processing: prospects in future biorefineries, Curr. Green Chem. 2 (2015) 90–95.
[5] S. Rama Mohan, Strategy and design of innovation policy road mapping for a waste biorefinery, Biores. Technol. 215 (2016) 76–83.
[6] A.M. Raspolli Galletti, C. Antonetti, E. Ribechini, M.P. Colombini, N. Nassi o Di Nasso, E. Bonari, From giant reed to levulinic acid and gamma-valerolactone: a high yield catalytic route to valeric biofuels, Appl. Energy 102 (2013) 157–162.
[7] A.M. Raspolli Galletti, C. Antonetti, V. De Luise, M. Martinelli, A sustainable process for the production of γ-valerolactone by hydrogenation of biomass-derived levulinic acid, Green Chem. 14 (2012) 688–694.
[8] S. Rivas, A.M. Raspolli Galletti, C. Antonetti, V. Santos, J.C. Parajó, Sustainable conversion of Pinus pinaster wood into biofuel precursor: a biorefinery approach, Fuel 164 (2016) 51–58.
[9] S. Rivas, A.M. Raspolli Galletti, C. Antonetti, V. Santos, J.C. Parajó, Sustainable production of levulinic acid from the cellulose fraction of Pinus pinaster wood: operation in aqueous media under microwave irradiation, J. Wood Chem. Technol. 35 (2015) 315–324.
[10] P.K. Rout, A.D. Nannaware, O. Prakash, A. Kalra, R. Rajasekharan, Synthesis of hydroxymethylfurfural from cellulose using green processes: a promising biochemical and biofuel feedstock, Chem. Eng. Sci. 142 (2016) 318–346.
[11] S.G. Wettstein, D.M. Alonso, E.I. Gürbüz, J.A. Dumesic, A roadmap for conversion of lignocellulosic biomass to chemicals and fuels, Curr. Opin. Chem. Eng. 1 (2012) 218–224.
[12] S.P. Teong, G. Yi, Y. Zhang, Hydroxymethylfurfural production from bioresources: past, present and future, Green Chem. 16 (2014) 2015–2026.
[13] A. Mukherjee, M. Dumont, V. Raghavan, Review: sustainable production of hydroxymethylfurfuarl and levulinic acid: challenges and opportunities, Biomass Bioenergy 72 (2015) 143–183.
[14] T. Wang, M.W. Nolte, B.H. Shanks, Catalytic dehydration of C6 carbohydrates for the production of hydroxymethylfurfural (HMF) as a versatile platform chemical, Green Chem. 16 (2014) 548–572.
[15] I. Agirrezabal-Telleria, I. Gandarias, P.L. Arias, Heterogeneous acid-catalysts for the production of furan-derived compounds (furfural and hydroxymethylfurfural) from renewable carbohydrates: a review, Catal. Today 234 (2014) 42–58.
[16] R.J. Van Putten, J.C. Van der Waal, E. De Jong, C.B. Rasrendra, H.J. Heeres, J.G. de Vries, Hydroxymethylfurfural, a versatile platform chemical made from renewable resources, Chem. Rev. 113 (2013) 1499–1597.
[17] R.L. De Souza, H. Yu, F. Rataboul, N. Essayem, 5-Hydroxymethylfurfural (5-HMF) production from hexoses: limits of heterogeneous catalysis in hydrothermal conditions and potential of concentrated aqueous organic acids as reactive solvent system, Challenges 3 (2012) 212–232.

[18] F. Yang, Q. Liu, X. Bai, Y. Du, Conversion of biomass into 5-hydroxymethylfurfural using solid acid catalyst, Biores. Technol. 102 (2011) 3424–3429.

[19] I. Van Zandvoort, Y. Wang, B.C. Rasrendra, E.R.H. van Eck, P.C.A. Bruijnincx, H.J. Heeres, B.M. Weckhuysen, Formation, molecular structure, and morphology of humins in biomass conversion: influence of feedstock and processing condition, ChemSusChem 6 (2013) 1745–1758.

[20] C. Antonetti, D. Licursi, S. Fulignati, G. Valentini, A.M. Raspolli Galletti, New frontiers in the catalytic synthesis of levulinic acid: from sugars to raw and waste biomass as starting feedstock, Catalysts 6 (2016) 196–224.

[21] F.N.D. Gomes, L.R. Pereira, N.F.P. Ribeiro, M.M.V.M. Souza, Production of 5-hydroxymethylfurfural (HMF) via fructose dehydration: effect of solvent and salting-out, Braz. J. Chem. Eng. 32 (2015) 119–126.

[22] F. Wang, H. Wu, C. Liu, R. Yang, W. Dong, Catalytic dehydration of fructose to 5-hydroxymethylfurfural over Nb$_2$O$_5$ catalyst in organic solvent, Carbohydr. Res. 368 (2013) 78–83.

[23] J. Zhang, A. Das, R.S. Assary, L.A. Curtiss, E. Weitz, A combined experimental and computational study of the mechanism of fructose dehydration to 5-hydroxymethylfurfural in dimethylsulfoxide using Amberlyst 70 PO$_4$$^{3-}$/niobic acid, or sulfuric acid catalysts, Appl. Catal. B: Environ. 181 (2016) 874–887.

[24] L. Lai, Y. Zhang, The production of 5-hydroxymethylfurfural from fructose in isopropyl alcohol: a green and efficient system, ChemSusChem 4 (2011) 1745–1748.

[25] J. Liu, Y. Tang, K. Wu, C. Bi, Q. Cui, Conversion of fructose into 5-hydroxymethylfurfural (HMF) and its derivatives promoted by inorganic salt in alcohol, Carbohydr. Res. 350 (2012) 20–24.

[26] Y. Xiao, Y. Song, Efficient catalytic conversion of fructose into 5-hydroxymethylfuran by heteropolyacids in the ionic liquid of 1-butyl-3-methyl imidazolium chloride, Appl. Catal. A: Gen. 484 (2014) 74–78.

[27] W. Liu, J. Holladay, Catalytic conversion of sugars into hydroxymethylfurfural in ionic liquids, Catal. Today 200 (2013) 106–116.

[28] V.V. Ordomsky, J. van der Shaaf, J.C. Schouten, T.A. Nijhuis, Fructose dehydration to 5-hydroxymethylfurfural over solid acidic catalysts in a biphasic system, ChemSusChem 5 (2012) 1812–1819.

[29] Y. Román-Leshkov, J.A. Dumesic, Solvent effect on fructose dehydration to 5-hydroxymethylfurfural in biphasic systems saturated with inorganic salts, Top. Catal. 52 (2009) 297–303.

[30] P. Wrigstedt, J. Keskiväli, T. Repo, Microwave-enhanced aqueous biphasic dehydration of carbohydrate to 5-hydroxymethylfurfural, RSC Adv. 6 (2016) 18973–18979.

[31] X. Zhang, D. Zhang, Z. Sun, L. Xue, X. Wang, Z. Jiang, Highly efficient preparation of HMF from cellulose using temperature-responsive heteropolyacid catalysts in cascade reaction, Appl. Catal. B: Environ. 196 (2016) 50–56.

[32] F.C. De Melo, R.F. De Souza, P.L.A. Coutinho, M.O. De Souza, Synthesis of 5-hydroxymethylfurfural from dehydration of fructose and glucose using ionic liquids, J. Braz. Chem. Soc. 25 (2014) 2378–2384.

[33] G. Morales, J.A. Melero, M. Paniagua, J. Iglesias, B. Hernández, M. Sanz, Sulfonic acid heterogeneous catalysts for dehydration of C$_6$-monosaccharides to 5-hydroxymethylfurfural in dimethyl sulfoxide, Chin. J. Catal. 35 (2014) 644–655.

[34] Q. Xinhua, M. Watanabe, T. Aida, R.L. Smith, Catalytic dehydration of fructose into 5-hydroxymethylfurfural by ion-exchange resin in mixed-aqueous system by microwave heating, Green Chem. 10 (2008) 799–805.

[35] J.S. Kruger, V. Nikolakis, D.G. Vlachos, Aqueous-phase fructose dehydration using Brönsted acid zeolites: catalytic activity of dissolved aluminosilicate species, Appl. Catal. A: Gen. 469 (2014) 116–123.

[36] V. Rac, V. Rakic, D. Stosic, O. Otman, A. Auroux, Hierarchical ZSM-5, beta and USY zeolites: acidity assessment by gas and aqueous phase calorimetry and catalytic activity in fructose dehydration reaction, Microporous Mesopourus Mater. 194 (2014) 126–134.

[37] T.D. Swift, H. Nguyen, Z. Erdman, J.S. Kruger, V. Nikolakis, D.G. Vlachos, Tandem Lewis acid/Brönsted acid-catalysed conversion of carbohydrates to 5-hydroxymethylfurfural using zeolite beta, J. Catal. 333 (2016) 149–161.

[38] F.S. Asghari, H. Yoshida, Dehydration of fructose to 5-hydroxymethylfurfural in sub-critical water over heterogeneous zirconium phosphate catalysts, Carbohydr. Res. 341 (2006) 2379–2387.

[39] C. Bastioli, L. Capuzzi, G. Carotenuto, A. Di Martino, A. Ferrari, Process for the production and isolation of 5-hydroxymethylfurfural, (2016) Patent WO 2016/059205 A1.

[40] F. Benvenuti, C. Carlini, P. Patrono, A.M. Raspolli Galletti, G. Sbrana, M.A. Massucci, P. Galli, Heterogeneous zirconium and titanium catalysts for the selective synthesis of 5-hydroxymethyl-2-furaldeyde from carbohydrates, Appl. Catal. A: Gen. 193 (2000) 147–153.

[41] C. Carlini, M.N. Giuttari, A.M. Raspolli Galletti, G. Sbrana, T. Armaroli, G. Busca, Selective saccharides dehydration to 5-hydroxymethyl-2-furaldehyde by heterogeneous niobium catalysts, Appl. Catal. A: Gen. 183 (1999) 295–302.

[42] P. Carniti, A. Gervasini, S. Biella, A. Auroux, Niobic acid and niobium phosphate as highly acidic viable catalyst in aqueous medium: fructose dehydration reaction, Catal. Today 118 (2006) 373–378.

[43] P. Khemthong, P. Daorattanachai, N. Laosiripojana, K. Faungnawakij, Copper phosphate nanostructure catalyse dehydration of fructose to 5-hydroxymethylfurfural, Catal. Commun. 29 (2012) 96–100.

[44] I. Jiménez-Morales, A. Teckchandani-Ortiz, J. Santamaría-González, P. Maireles-Torres, A. Jiménez-López, Selective dehydration of glucose to 5-hydroxymethylfurfural on acidic mesoporous tantalum phosphate, Appl. Catal. B: Environ. 144 (2016) 22–28.

[45] Y. Zhang, J. Wang, J. Ren, X. Liu, X. Li, Y. Xia, G. Lu, Y. Wang, Mesoporous niobium phosphate: an excellent solid acid for the dehydration of fructose to 5-hydroxymethylfurfural in water, Catal. Sci. Technol. 2 (2012) 2485–2491.

[46] R.M. West, D.J. Braden, J.A. Dumesic, Dehydration of butanol to butane over solid acid catalysts in high water environments, J. Catal. 262 (2009) 134–143.

[47] P. Carniti, A. Gervasini, F. Bossola, V. Dal Santo, Cooperative action of Brønsted and Lewis acid sites of niobium phosphate catalysts for cellobiose conversion in water, Appl. Catal. B: Environ. 193 (2016) 93–102.

[48] I. Nowak, M. Ziolek, Niobium compounds: preparation, characterization, and application in heterogeneous catalysis, Chem. Rev. 99 (1999) 3603–3624.

[49] A. Jain, A.M. Shore, S.C. Jonnalagadda, K.V. Ramanujachary, A. Mugweru, Conversion of fructose, glucose and sucrose to 5-methyl-2-furaldehyde over mesoporous zirconium phosphate catalyst, Appl. Catal. A: Gen. 489 (2015) 72–76.

[50] A. Richel, P. Laurent, B. Wathelet, J. Wathelet, M. Paquot, Microwave-assisted conversion of carbohydrates: state of art and outlook, C. R. Chim. 14 (2011) 224–234.

[51] A.M. Raspolli Galletti, C. Antonetti, M. Bertoldo, F. Piccinelli, Chitosan as biosupport for the MW-assisted synthesis of palladium and their use in the hydrogenation of ethyl cinnamate, Appl. Catal. A: Gen. 468 (2013) 95–101.

[52] A.M. Raspolli Galletti, C. Antonetti, M. Marracci, F. Piccinelli, B. Tellini, Novel microwave-synthesis of Cu nanoparticles in the absence of any stabilizing agents and their antibacterial and antistatic applications, Appl. Surf. Sci. 280 (2013) 610–618.

[53] Y. Kamiya, S. Sakata, Y. Yoshinaga, R. Ohnishi, T. Okuhara, Zirconium phosphate with a high surface area as a water-tolerant solid acid, Catal. Lett. 94 (2004) 45–47.

[54] G. Gliozzi, A. Innorta, A. Mancini, R. Bortolo, C. Perego, M. Ricci, F. Cavani, Zr/P/O catalyst for the direct acid chemo-hydrolysis of non-pretreated microcrystalline cellulose and softwood sawdust, Appl. Catal. B: Environ. 145 (2014) 24–33.

[55] A.L. Ginestra, P. Patrono, Acidic properties of Ge, Ti Zr and Sn phosphates and arsenates, Mater. Chem. Phys. 17 (1987) 161–179.

[56] S.M. Patel, U.V. Chudasama, P.A. Ganeshpure, Cyclodehydration of 1,4-butanediol catalyzed by metal(IV) phosphates, React. Kinet. Catal. Lett. 76 (2002) 317–325.

[57] T. Hattori, A. Ishiguro, Y. Murakami, Acidity of crystalline zirconium phosphate, J. Inorg. Nucl. Chem. 40 (1978) 1107–1111.

[58] D. Spielbauer, G.A.H. Mekhemer, T. Riemer, M.I. Zaki, H. Knözinger, Structure and acidic properties of phosphate-modified zirconia, J. Phys. Chem. B 101 (1997) 4681–4688.

[59] T. Armaroli, G. Busca, C. Carlini, M. Giuttari, A.M.R. Galletti, G. Sbrana, Acid sites characterization of niobium phosphate catalysts and their activity in fructose dehydration to 5-hydroxymethyl-2-furaldehyde, J. Mol. Catal. A 151 (2000) 233–243.

[60] W. Alharbi, E. Brown, E.F. Kozhevnikova, I.V. Kozhevnikov, Dehydration of ethanol over heteropoly acid catalysts in the gas phase, J. Catal. 319 (2014) 174–181.

[61] V.V. Ordomsky, V.L. Sushkevich, J.C. Schouten, J. Van der Schaaf, T.A. Nijhuis, Glucose dehydration to 5-hydroxymethylfurfural over phosphate catalyst, J. Catal. 300 (2013) 37–46.

[62] A.S. Rocha, A.M.S. Forrester, M.H.C. De la Cruz, C.T. Da Silva, E.R. Lachter, Comparative performance of niobium phosphates in liquid phase anisole benzylation with benzyl alcohol, Catal. Commun. 9 (2008) 1959–1965.

[63] M. Helen, B. Viswanathan, S.S. Murthy, Synthesis and characterization of composite membranes based on α-zirconium phosphate and silicotungstic acid, J. Membr. Sci. 292 (2007) 98–105.

[64] B.A. Fachri, R.M. Abdilla, H.H. Van de Bovenkamp, C.B. Rasrendra, H.J. Heeres, Experimental and kinetic modeling studies on the sulfuric acid catalyzed conversion of D-fructose to 5-hydroxymethylfurfural and levulinic acid in water, ACS Sustain. Chem. Eng. 3 (2015) 3024–3034.

[65] H. Xu, Z. Miao, H. Zhao, J. Yang, J. Zhao, H. Song, N. Liang, L. Chou, Dehydration of fructose into 5-hydroxymethylfurfural by high stable ordered mesoporous zirconium phosphate, Fuel (2015) 234–240.

[66] A. Ranoux, K. Djanashvili, I.W.C.E. Arends, U. Hanefeld, 5-Hydroxymethylfurfural synthesis from hexose is autocatalytic, ACS Catal. 3 (2013) 760–763.

[67] S. Rivas, J. González-Muñoz, V. Santos, J.C. Parajó, Acidic processing of hemicellulosic saccharides of pine wood: product distribution and kinetic modelling, Biores. Technol. 162 (2014) 192–199.

[68] M. Möller, P. Nilges, F. Harnisch, U. Schröder, Subcritical water as reaction environment: fundamentals of hydrothermal biomass transformation, ChemSusChem 4 (2011) 566–579.

[69] T. Flannelly, M. Lopes, L. Kupiainen, S. Dooley, J.J. Leahy, Non-stoichiometric formation of formic acid and levulinic acid from the hydrolysis of biomass derived hexose carbohydrates, RSC Adv. 6 (2016) 5797–5804.

[70] B.A. Fachri, R.M. Abdilla, C.B. Rasrendra, H.J. Heeres, Experimental and modelling studies on the acid-catalyzed conversion of inulin to 5-hydroxymethylfurfural in water, Chem. Eng. Res. Des. 109 (2016) 65–75.

[71] S. Wang, H. Lin, Y. Zhao, J. Chen, J. Zhou, Structural characterization and pyrolysis behaviour of humin by-products from the acid-catalyzed conversion of C6 and C5, J. Anal. Appl. Pyrolysis 118 (2016) 259–266.

[72] C.S. Rasrendra, M. Windt, Y. Wang, S. Adisasmito, I.G.B.N. Makertihartha, E.R.H. Van Eck, D. Meier, H.J. Heeres, Experimental studies on the pyrolysis of humins from the acid-catalysed dehydration of C6-sugars, J. Anal. Appl. Pyrolysis 104 (2013) 299–307.

[73] A. Chuntanapum, Y. Matsumura, Formation of tarry material from 5-HMF in subcritical and supercritical water, Ind. Eng. Chem. Res. 48 (2009) 9837–9846.

[74] M. Tatzber, M. Stemmer, H. Spiegel, C. Katzlberger, G. Haberhauer, A. Mentler, M.H. Gerzabek, FTIR-spectroscopic characterization of humic acids and humin fractions obtained by advanced NaOH Na$_4$P$_2$O$_7$, and Na$_2$CO$_3$ extraction procedures, J. Plant Nutr. Soil Sci. 170 (2007) 522–529.